# Mechanical behaviour analysis of a high strength steel using acoustic emission technique

Anghel-Vasile Cernescu

## 1. Introduction

Acoustic emission (AE) is understood as the elastic waves generated by abrupt changes in the internal stress field of a body. Such changes of local stress may occur from natural phenomena such as dislocation motion, crack growth and martensitic phase transformation, [1]. Starting from this concept of defining the acoustic emission, this technique is typically used in the evaluation and localization of the material damage, regardless of its nature or type of degradation. Sharma and Parey, [2 – 5], have published a series of papers in which mathematical models are developed to predict the AE energy. Through an association of the electrical signal with the elastic strain energy, predictions of AE RMS could be made based on the geometric and functional parameters of an involute spur gear pair or a rolling bearing. An analytical model for prediction of AE RMS in turning operations is proposed in Ref. [6]. AE RMS have been observed to increase with the increase of cutting speed, cutting force and shear plane angle and respectively decrease with the increase in positive rake angle of the tools.
Based on a comparative analysis of some AE parameters, Harris and Bell, [7], present a series of conclusions, from which it can be mentioned that: 1) the energy rate can be superior to count rate in the continuous emission; 2) the AE RMS voltages appeared to be closely related to the strain rate; 3) a linear relation between counts and energy was observed in fracture toughness respectively fatigue crack growth tests. Through the parameters of the acoustic emission, this technique allows the identification and even the localization of any structural modification of the material that has a consequence in the emission of elastic stress waves. Thus, the number of counts and the counting rate respectively can be associated with stress corrosion, stress cracking, hydrogen embrittlement and mechanical and fracture behaviour of metals, ceramics and composites. The AE RMS value can be used to measure the AE activity and hence size of dislocation and severity of damage. In general, the AE energy can be associated with mechanical energy. Energy signal gives substantially the same information as the counting rate. Acoustic emission generated during the Luders band elongation of water quenched and tempered medium carbon has been studied by Haneef et all., [8]. AE RMS is found to decrease with tempering due to lower yield stress ferrite grain growth. Specific predominant frequencies were observed in both the quenched and tempered samples. The predominant frequencies specific to tempered samples being lower than those of water quenched samples. According to Haneef et all., [9], AE generated during tensile deformation of metallic materials with single-phase microstructure records a peak at strain levels corresponding to yielding zone. The AE activity is mainly generated by the formation of dislocations. Also, in the linear elastic region waveform signals are generated at two dominant frequencies which are independent of strain rate. The AE RMS voltage increase with increase in strain rate due to the increase in source activation and AE dominant frequency increase from elastic region to around 590 kHz during strain hardening and 710 kHz around the ultimate tensile strength.
Despite of studies linking the acoustic emission parameters to different mechanical processes that occur at the structural level, there is a lack of correlation of AE parameters with properties of mechanical behaviour of materials, such as strain energy. In this paper, the AE parameters that can be correlated with the strain energy accumulated in the material during a tensile loading will be checked. Also, the AE activity of a martensite high strength steel will be analysed in correspondence with its mechanical behaviour.

## 2. Materials and methods

### *2.1. Tensile tests on high strength steel*

Tensile tests were performed on a high strength structural steel Weldox 960 quenched and tempered, [10], in which the acoustic emission signals were recorded using sensors mounted on each sample. The tests were performed according to BS EN 10002-1:2001 standard on a 100 kN Zwick electromechanical testing machine, fig. 1. Aluminium tabs were glued on the sample gripping parts to avoid slipping into the jaws but also to reduce the noise in the recorded signals, fig. 2. The acoustic signals were recorded by two sensors, Nano 30, each connected to a Mistras 2/4/6 preamplifier. The preamplifiers were also connected to a Mistras AE System, controlled by AEwin software.

Weldox 960 is a BCC structure, lath martensite steel, with high strength properties associated with high ductility.


Fig. 1. The tensile testing rig

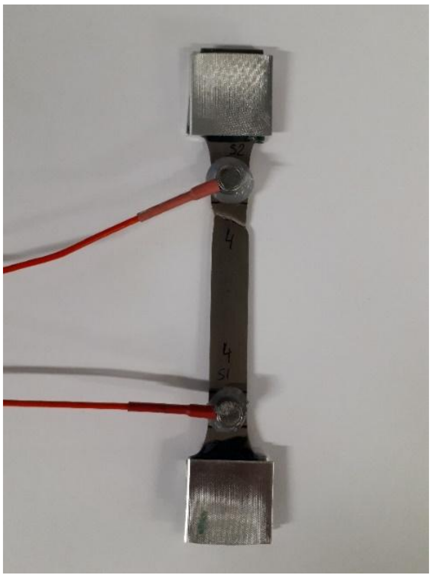

Fig. 2. Tensile specimen with aluminium tabs

### *2.2. Correlation methods*

Generally, the correlation is a statistical tool used to measure the strength association between two variables and the direction of the relationship, [11 - 14]. The strength of relationship between variables is defined by a correlation coefficient which varies from -1 to +1. A value of ±1 indicates a perfect degree of association. As the correlation coefficient goes towards 0, the relationship between the two variables will be weaker, [11]. Two correlation methods have been used in this paper to verify the relationship between the strain energy accumulated during tensile loading and the AE accumulated absolute energy, respectively. The two methods are the Pearson and Spearman correlation.

*Pearson correlation*, $r_{xy}$, is a number that indicates the extent to which two variables are linearly related. Basically, a Pearson product-moment correlation indicates how far the data points are to the line of best fit. The following formula can be used to calculate the Pearson correlation:

$$r_{xy} = \frac{n\sum x_i y_i - \sum x_i \sum y_i}{\sqrt{n\sum x_i^2 - (\sum x_i)^2} \cdot \sqrt{n\sum y_i^2 - (\sum y_i)^2}} \quad (1)$$

where $n$ is the number of observations, $x_i$ is the value of $x$ variable, $y_i$ is the value of $y$ variable.

The Pearson correlation requires the following data assumptions to hold: interval or ratio level, linearly related and bivariate normally distributed. If the variables do not meet the above assumptions, then the Spearman's rank correlation must be used.
*Spearman's correlation*, $r_s$, is a statistical measure of the strength of a monotonic relationship between paired data. A monotonic function is one that either never increases or never decreases as its independent variable increases. Monotonically increasing function appear when the independent variable increases, and the dependent variable never decreases. Monotonically decreasing function appear when the increase of the independent variable determines the increasing of the dependent variable. The third case covered by the Spearman's correlation is the non-monotonic function when the increasing of the independent variable will cause sometimes decreasing of the dependent variable and sometimes increasing of it. The calculation of Spearman's correlation coefficient requires the following data assumptions to hold: interval or ratio level or ordinal and monotonically related. The following formula can be used to calculate the Spearman rank correlation:

$$r_s = 1 - \frac{6\sum d_i^2}{n(n^2-1)} \qquad (2)$$

where $d_i$ is the difference between the ranks of corresponding variables and $n$ is the number of observations.

## 3. Results and discussion

The mechanical behaviour of Weldox 960 steel is highlighted on the characteristic stress-strain curve. The material exhibits a linear elastic behaviour up to the yield limit, followed by a portion with plastic deformation until the maximum strength. The plastic deformation is characterized by a low hardening coefficient, which can be easily approximated by a linear variation. Once the ultimate strength is reached, the sample begin to strangle, the material behaviour being characterized by a plastic softening until the final fracture. Figure 3.a shows the experimental stress-strain curves and also based on the ASTM E646 standard, [15], the true stress-true strain curves were determined, fig. 3.b. At the same time, using these curves a Ramberg-Osgood equation, given by the equation (3), was fitted. The mechanical properties of the analysed steel as well as the coefficients of the Ramberg-Osgood equation are presented in Table 1.

$$\varepsilon_{true} = \frac{\sigma_{true}}{E} + \left(\frac{\sigma_{true}}{K}\right)^{\frac{1}{n}} \qquad (3)$$

where $\sigma_{true}$ is the true stress, $\varepsilon_{true}$ is the corresponding true strain, $K$ is the strength coefficient, $n$ is the strain hardening exponent.

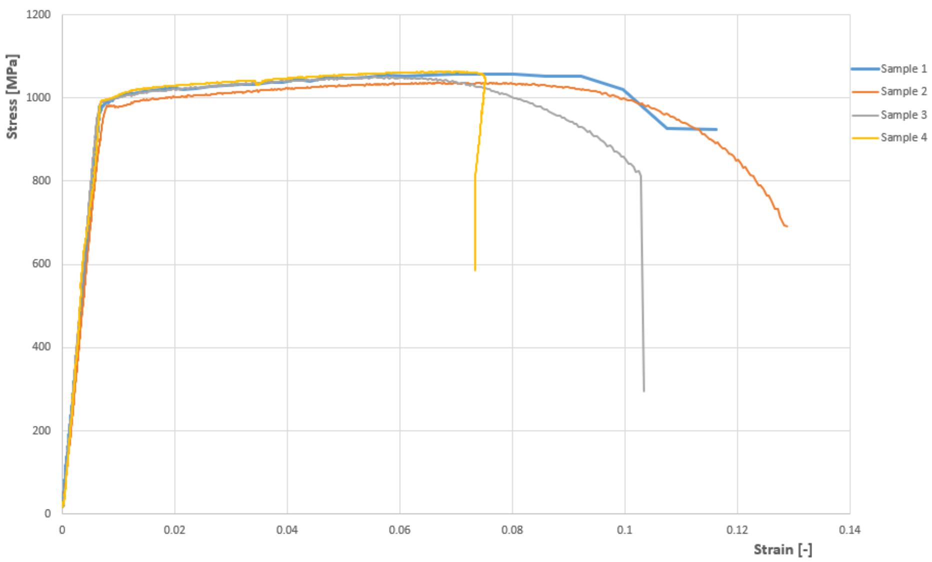


a)

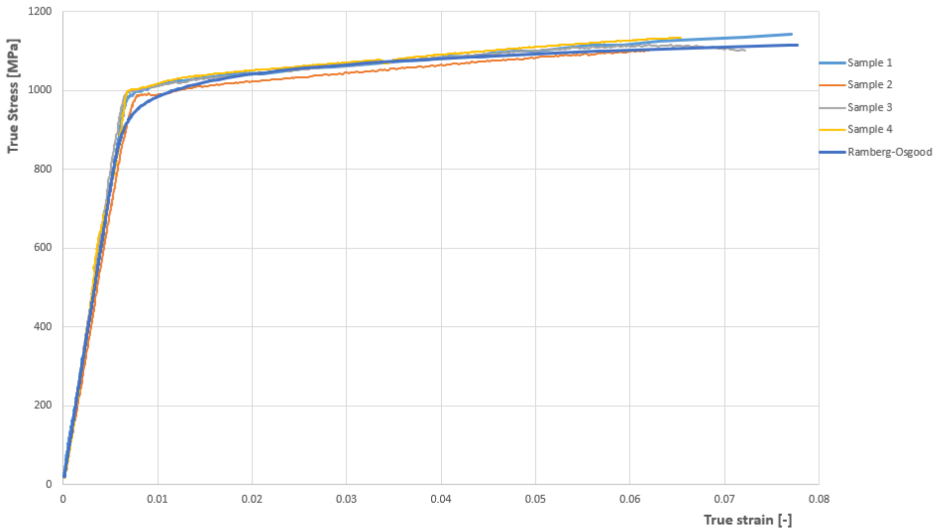


b)

Fig. 3. The mechanical behaviour of Weldox 960 steel: a) engineering stress-strain curves; b) true stress-true strain curves.

**Table 1**. The mechanical properties of Weldox 960 steel

| **Material** | **Young's modulus [MPa]** | **Yield strength [MPa]** | **Ultimate Strength [MPa]** | **Ramberg-Osgood coefficients** | |
|---|---|---|---|---|---|
| | | | | **K [MPa]** | **n** |
| Weldox 960 steel | 202000 | 960 | 1052 | 1246.58 | 0.0416 |

The initial state of a body in which no external forces are applied is a thermodynamically equilibrium condition called a *natural state*. The energy in the natural state is termed $E_0$. When external forces are applied to a body, the energy state $E_1$ of the body is increased due to the disturbance of the natural state. If the external forces are unloaded, the natural state is recovered and the difference $\Delta E$ between $E_1$ and $E_0$ can be written as:

$$\Delta E = E_1 - E_0 \tag{4}$$

Usually, $\Delta E = dU$ is called the *elastic strain energy* per unit volume and it is expressed in terms of stresses and strains in a body, [16]:

$$dU = \frac{1}{2}\left(\sigma_x \varepsilon_x + \sigma_y \varepsilon_y + \sigma_z \varepsilon_z + \tau_{xy}\gamma_{xy} + \tau_{yz}\gamma_{yz} + \tau_{zx}\gamma_{zx}\right) dx \cdot dy \cdot dz \quad (5)$$

The product $dx{\cdot}dy{\cdot}dz$ represents the volume of an elementary unit in the loaded body.

In the case of a tensile loading, the stress state is uniaxial and the expression (5) is reduced to:

$$dU = \frac{1}{2}\sigma_x \varepsilon_x \cdot dx \cdot dy \cdot dz \quad (6)$$

If the Hooke's law is considered and relate the axial strain to the axial stress through the elasticity Young's modulus, it results:

$$dU = \frac{1}{2}\sigma_x \frac{\sigma_x}{E} \cdot dx \cdot dy \cdot dz = \frac{\sigma_x^2}{2E} \cdot V \quad (7)$$

where $V = dx{\cdot}dy{\cdot}dz$ is the volume of the axially loaded body.

Looking at relations (6) and (7) and associating with the stress-strain curve from tensile loading, it can be observed that the strain energy represents the area covered by the trajectory of the curve. Thus, on the linear-elastic domain, relation (6) represents the area of a triangle formed under the stress-strain curve, at a certain level of the stress, fig. 4.a. Once the material begins to plastically deform a release (dissipation) of an amount of strain energy takes place. Therefore, the total strain energy at a certain level of stress, in the elastic-plastic domain, is composed of an amount of elastic strain energy and an amount of strain energy released (dissipated), fig. 4.b.

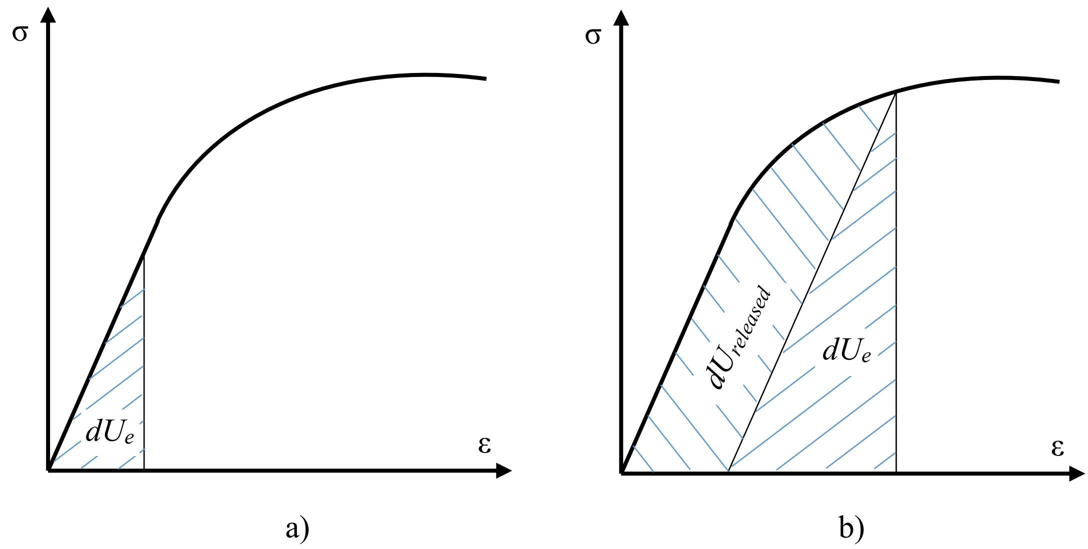


Fig. 4. The strain energy illustration on tensile loading: a) elastic strain energy; b) strain energy corresponding to plastic deformation.

Considering this approach in the tensile tests of Weldox 960 steel, the strain energy was determined by evaluating the area delimited by the true stress – strain curve. Figure 5 shows the total and elastic strain energy depending on the true stress, represented on the semi-logarithmic scale. In all four samples, the total strain energy, determined based on the area evaluation, correlates well with the elastic strain energy, determined based on the relation (7), up to the yield limit. Once the yield limit is exceeded, the material enters the plastic deformation field characterized by a large amount of strain energy released. Thus, the total strain energy increases much compared to the elastic strain energy.

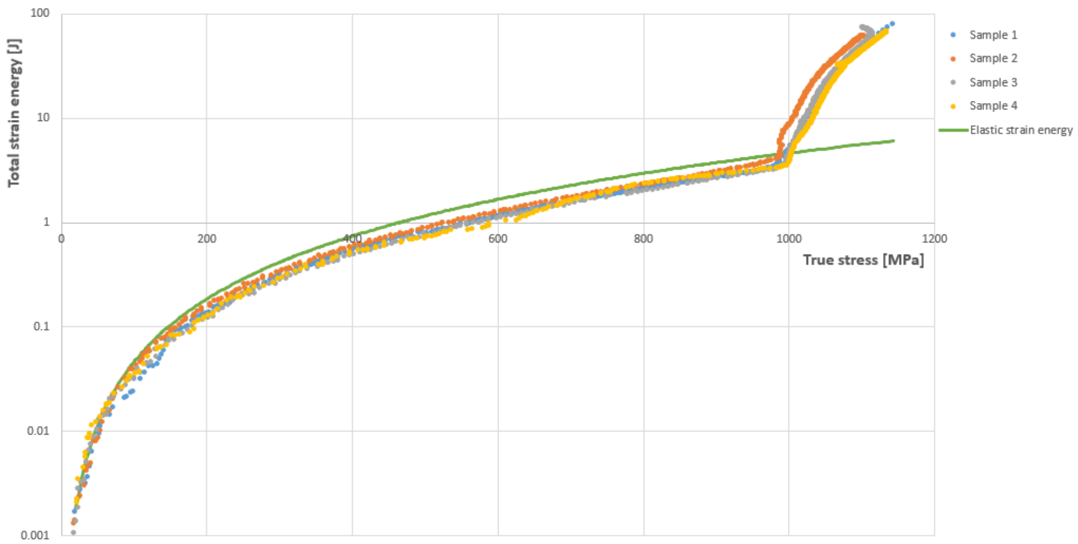


Fig. 5. The strain energy in function of the true stress from tensile tests on Weldox 960 steel

Regarding the AE signal, the variations of AE RMS and Accumulated Absolute Energy in function of the tensile strain, are presented in Figures 6 and 7. In all cases, the AE RMS records high values in the yielding region characterized by the formation of Luders slip bands.

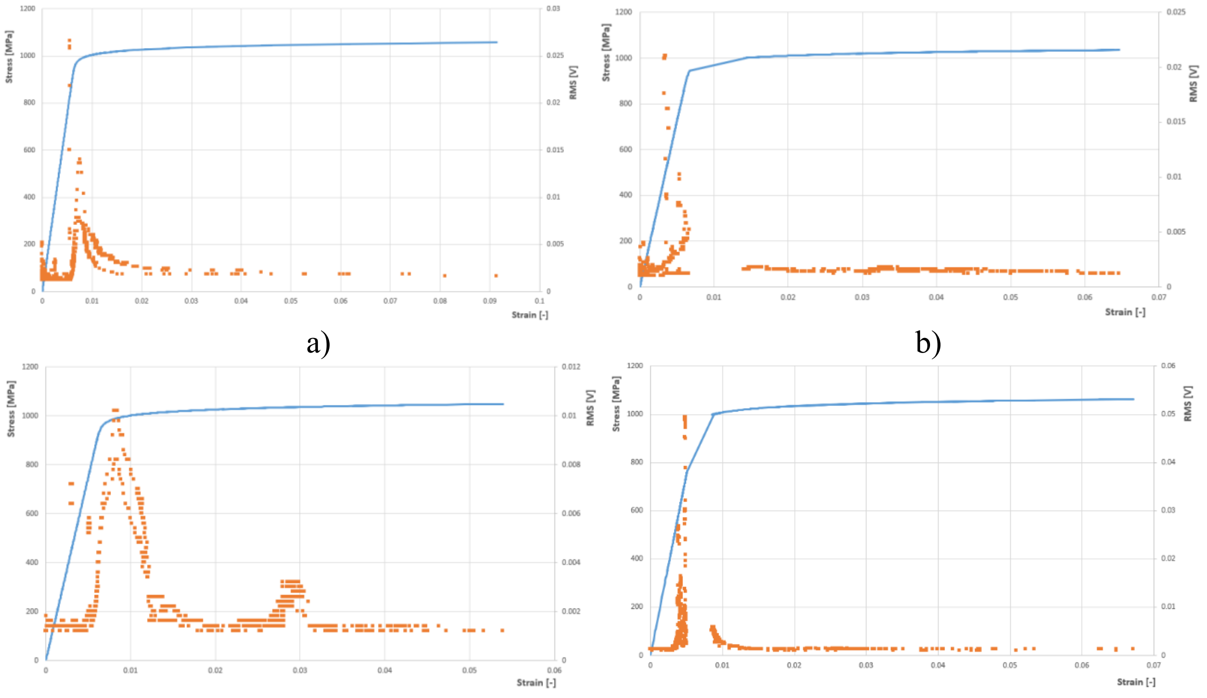


a) b)

c) d)

Fig. 6. The AE RMS in tensile tests: a) Specimen 1; b) Specimen 2; c) Specimen 3; d) Specimen 4.

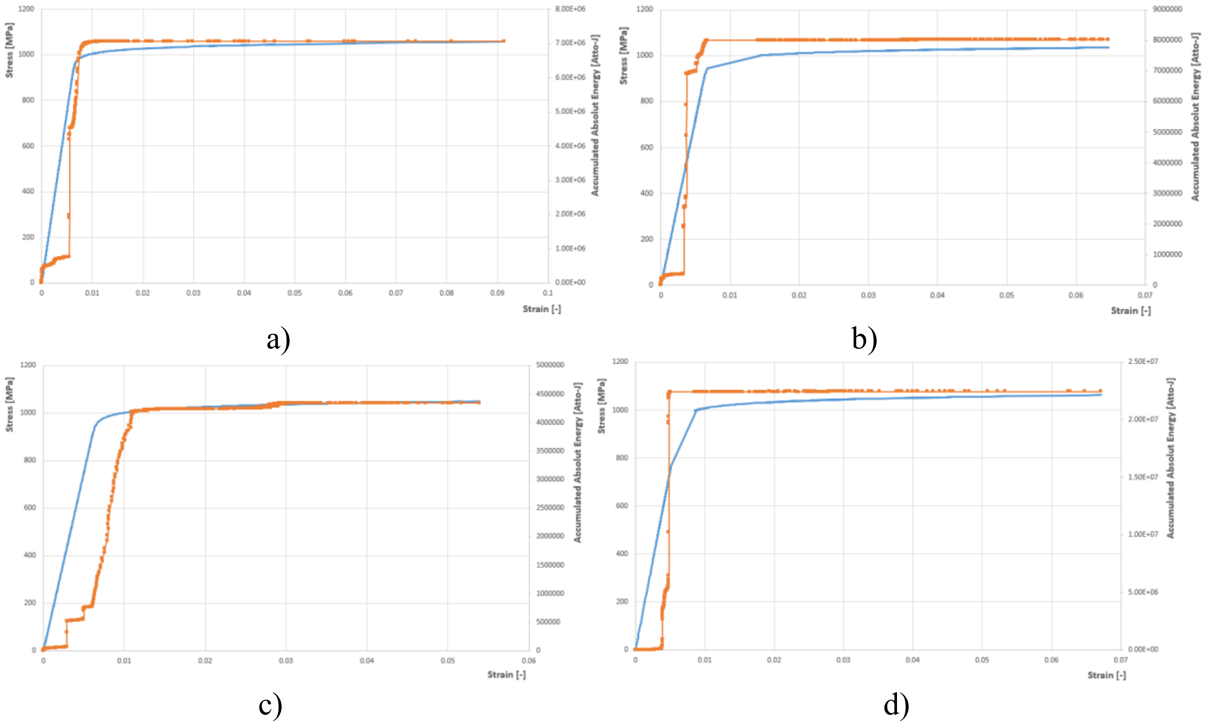


Fig. 7. The AE Accumulated Absolut energy in tensile tests: a) Specimen 1; b) Specimen 2; c) Specimen 3; d) Specimen 4.

Three types of variations of the AE RMS were observed in the yielding region, during the tensile tests. These variations reflect the initiation and propagation of the Luders bands on the one hand, but also the energy released for their formation.

First variation, fig. 8.a, was observed in samples 1 and 3 and describes four area with specific characteristics of AE RMS. Zone I starts with a high value (a jump) of AE RMS announcing the initiation of Luders bands. Once the process is started, the formation of the slip bands propagates along the following three zones with different rates. Zone II is characterized by gradually increase of AE RMS until the material yield strength is reached. In zone III, the formation of Luders bands with a higher rate continues until the maximum value of AE RMS is reached. Zone IV also continues with the formation of Luders bands but with a gradual decrease of the AE RMS until a saturation level is reached, where the entire gage length is covered by Luders bands. The decrease of AE RMS can be associated with the yield phenomenon.

Also, following the variation of AE RMS it is observed that after each increase a drop follows at almost the same strain. Based on this behaviour, in Figure 9 two values that reflect the formation of Luders bands in the yielding region are defined. Thus, the ΔAE RMS value corresponds to the formation of new bands and the AE $RMS_{drop}$ represents the energy released for the formation of new Luders bands. These two values are represented in function of the tensile strain, fig. 10.a and b. Following the two plots, it is observed that the ΔAE RMS value oscillates around 0.004 V during zones II to IV. Instead, the AE $RMS_{drop}$ remains constant in zone II, increase almost linearly in zone III and again stabilizes and remains constant in zone IV. The oscillating variation of ΔAE RMS can be explained by the number of Luders bands formed during one strain increment. It is assumed that in the yielding zone, each increment of the strain is followed by the formation of a pack of slip bands with different densities, and this is reflected in the variation of ΔAE RMS. Also, the AE $RMS_{drop}$ is the released energy to form a package of slip bands.

Also, in the case of samples 2 and 4, the AE RMS variations shows an "increases-drops" type character in the region of material yielding or just before it. Although it has different features, the AE RMS variation signals the initiation and propagation of the Luders slip bands until reach a saturation level. The results of these tests are consistent with similar observations reported by Haneef et al., [8, 9], or Petit at al., [17].

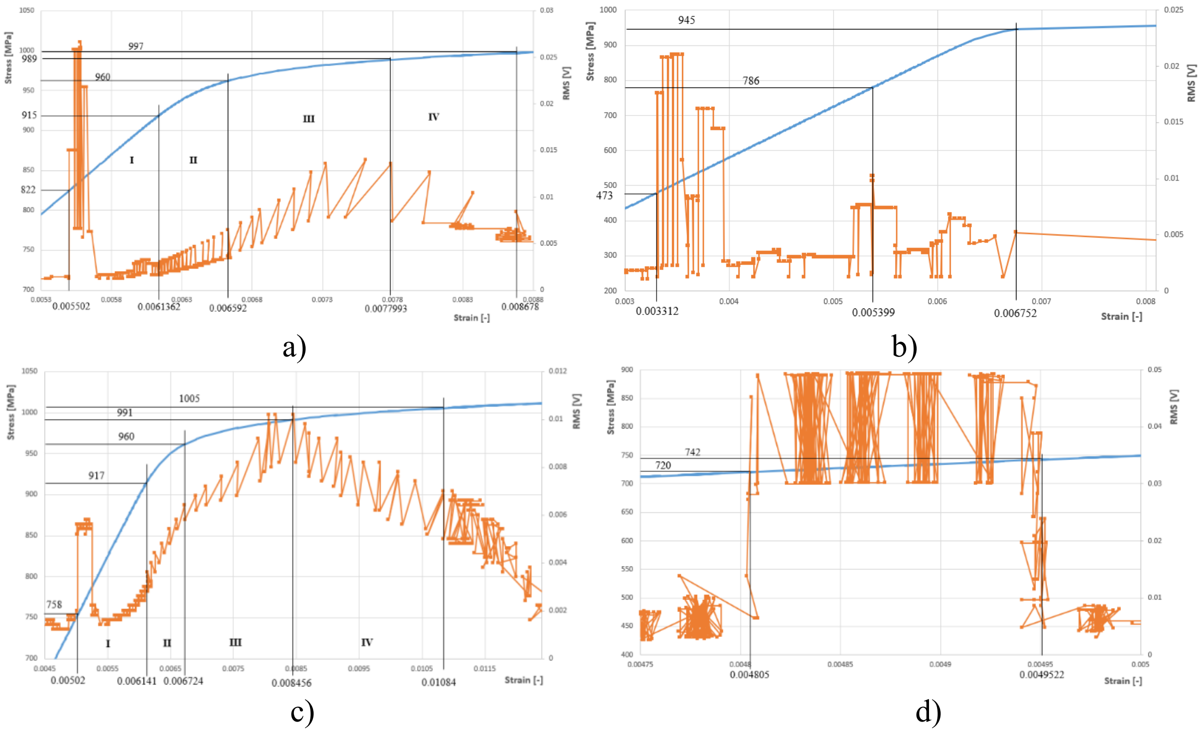


Fig. 8. The AE RMS variation in the yielding region: a) Specimen 1; b) Specimen 2; c) Specimen 3; d) Specimen 4

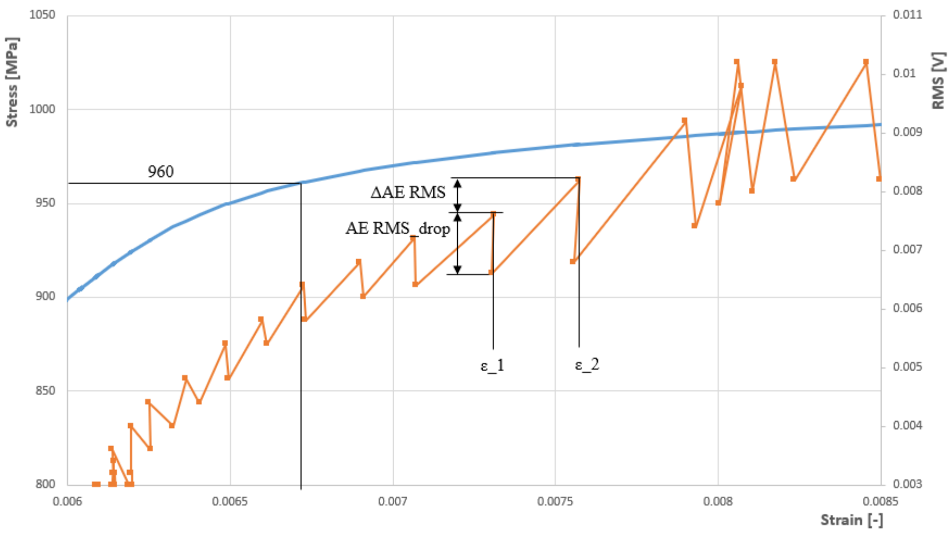


Fig. 9. Definition of two characteristics in the AE RMS variation

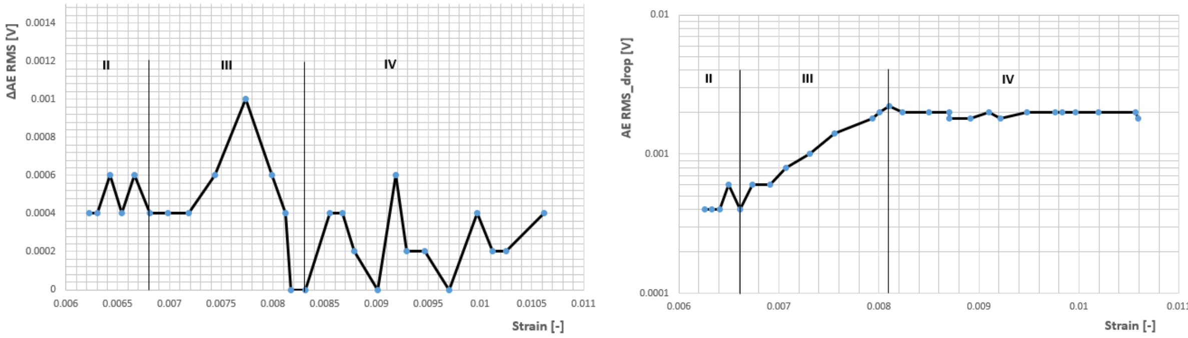


a) b)

Fig. 10. The variation of ΔAE RMS (a) and AE $RMS_{drop}$ (b) for Specimen 3.

The AE accumulated absolute energy shows a trend like a stress-strain curve. This parameter represents the cumulative energy of the acoustic signal during the entire tensile loading. Thus, Table 2 shows the degree of correlation of this AE parameter with the mechanical strain energy, by means of the Pearson and Spearman coefficients.

**Table 2**. The correlation coefficients of AE accumulated energy with the strain energy

| | Specimen 1 | | Specimen 2 | | Specimen 3 | | Specimen 4 | |
|---|---|---|---|---|---|---|---|---|
| | AE Acc. Abs. Energy compared to $dU_{total}$* | AE Acc. Abs. Energy compared to $dU_{el}$ | AE Acc. Abs. Energy compared to $dU_{total}$* | AE Acc. Abs. Energy compared to $dU_{el}$ | AE Acc. Abs. Energy compared to $dU_{total}$* | AE Acc. Abs. Energy compared to $dU_{el}$ | AE Acc. Abs. Energy compared to $dU_{total}$* | AE Acc. Abs. Energy compared to $dU_{el}$ |
| Pearson | 0.5914 | 0.8931 | 0.4284 | 0.8769 | 0.7795 | 0.9392 | 0.5531 | 0.9325 |
| Spearman | 0.9982 | 0.99825 | 0.9919 | 0.9925 | 0.9849 | 0.9899 | -0.0524 | -0.0421 |

*$dU_{total} = dU_{el} + dU_{released}$

The results indicate a low level of linear correlation between the analysed quantities, instead a very high level of monotonically increase of their dependence. Exception makes sample 4, where the Spearman coefficient is very low, and which could be due to a contamination of the acoustic signal.

This means that during tensile loading, the AE accumulated absolute energy increases with the strain energy accumulation.

This study shows the potential of the acoustic emission technique for investigating transient phenomena of mechanical loadings, the accumulation of strain energy in solid bodies and the monitoring of structural changes of loaded materials (such as permanent strain and crack initiation).

**Acknowledgement**

This study was supported by the project grant **FADAMES no. 792652**, funded by **Marie Curie Individual Fellowship Program** from Horizon 2020, European Commission.

**References**

[1] Y. Berlinsky, M. Rosen, J. Simmons, H.N.G. Wadley, *A calibration approach to acoustic emission energy measurement*, Journal of Nondestructive Evaluation, 10(1): 1 – 5, 1991;

[2] R.B. Sharma, A. Parey, *Modelling of acoustic emission generated by crack propagation in spur gear*, Engineering Fracture Mechanics, 182: 215 – 228, 2017;

[3] R.B. Sharma, A. Parey, *Modelling of acoustic emission generated due to pitting on spur gear*, Engineering Failure Analysis, 86: 1-20, 2018;
[4] R.B. Sharma, A. Parey, N. Tandon, *Modelling of acoustic emission generated in involute spur gear pair*, Journal of Sound and Vibration, 393: 353 – 373, 2017;
[5] R.B. Sharma, A. Parey, *Modelling of acoustic emission generated in rolling element bearing*, Applied Acoustics, 144: 96 – 112, 2019;
[6] D.P. Saini, Y.J. Park, *A quantitative model of acoustic emissions in orthogonal cutting operations*, Journal of Materials Processing Technology, 58: 343-350, 1996;
[7] D.O. Harris, R.L. Bell, *The measurement of energy in acoustic-emission testing*, Experimental Mechanics, p. 347 – 353, 1977;
[8] T.K. Haneef, C.K. Mukhopadhyay, B.P.C. Rao, T. Jayakumar, *Acoustic emissions generated during Luders band elongation of tempered medium carbon steel*, Strength, Fracture and Complexity, 6: 149-159, 2010;
[9] T. Haneef, B.B. Lahiri, S. Bagavathiappan, C.K. Mukhopadhyay, J. Philip, B.P. Chandra Rao, T. Jayakumar, *Study of the tensile behaviour of AISI type 316 stainless steel using acoustic emission and infrared thermography techniques*, Journal of Mater. Res. Technol., 4(3): 241-253, 2015;
[10] Weldox 960 – Data sheet, SSAB Oxelosund;
[11] https://www.statisticssolutions.com/correlation-pearson-kendall-spearman/ ;
[12] S. Adrian-Martines, M. Ardid, M. Bou-Cabo, I. Felis, C. Llorens, J.A. Martines-Mora, M. Saldana, *Acoustic signal detection through the cross-correlation method in experiments with different signal to noise ratio and reverberation conditions*, Cornell University, https://arxiv.org/abs/1502.05038 , 2015;
[13] D. Lyon, *The discrete Fourier Transform, Part 6: Cross-Correlation*, Journal of Object Technology, vol. 9, No. 2, pp. 17-22, 2010;
[14] G. Zhang, R.J. Doviak, J. Vivekanandan, W.O.J. Brown, S.A. Cohn, *Cross-correlation ratio method to estimate cross-beam wind and comparison with a full correlation analysis*, Radio Science, vol. 38, No. 3, 8052, 2003;
[15] ASTM E646, *Standard test method for tensile strain-hardening exponents (n-values) of metallic sheet materials*, ASTM International, USA;
[16] Y. Murakami, *Theory of elasticity and stress concentration*, John Wiley & Sons, Ltd, ISBN 9781119274131, 2017;
[17] J. Petit, D. Wagner, N. Ranc, G. Montay, M. Francois, *Comparison of different techniques for monitoring of the Luders bands development*, https://www.researchgate.net/profile/Guillaume_Montay/publication/286799373_Comparison_of_different_techniques_for_the_monitoring_of_the_Luders_bands_development/links/56935a6b08aec14fa55ded41.pdf;